QUENCH PROTECTION WITH LHC BEAM LOSS MONITORS

M. Sapinski*, B. Dehning, E. Effinger, J. Emery, E.B. Holzer, C. Kurfuerst, A. Priebe, C. Zamantzas,
CERN, Geneva, Switzerland

Abstract

To prevent from beam-induced quenches of the superconducting magnets a system of about 4000 beam loss detectors is installed on the magnets cryostat. These detectors, being ionisation chambers, measure the particle shower starting inside the magnet. Examples of simulations linking the heat deposited in the superconducting coils with signals in the ionisation chambers are presented. A comparison of the simulations to the data is done. Limits of the present system are discussed.

INTRODUCTION

The Beam Loss Monitor (BLM) system uses mainly cylindrical ionisation chambers, installed in various locations on the LHC, as radiation detectors. Most of the chambers are installed on the cryostat of the superconducting magnets. Their main goal is to detect if the energy deposition in the superconducting coil due to beam losses is high enough to provoke a transition of the coil to a normal-conducting state (quench). If the BLM system detects such a loss it sends a signal to the beam dump and the beam is removed from the LHC ring within 4 revolutions.

The beam-abort thresholds set up in BLM electronics [1] are a function of beam energy and signal integration time. Because the temporal and spatial distribution of the loss have a large impact on threshold, usually the most conservative values are chosen.

Various aspects of quench-protecting threshold estimations, which authors found especially interesting, are discussed in this paper.

METHOD

The ingredients needed to estimate the beam-abort thresholds are:

- beam loss distribution,

- quench margin of the magnet,

- energy deposited in the coil,

- signal in the BLM.

In the following, the four ingredients are discussed in detail.

---
* mariusz.sapinski@cern.ch

Beam Loss Distribution

The distribution of the beam losses depend on the trajectories of the particles and on the aperture of the vacuum chamber. An example of the loss pattern, obtained from SixTrack [2] simulation of beam halo particles, is shown in Figure 1, where the beam goes from left to right. To obtain this plot losses over all arcs were superimposed according to MB-MQ interconnection geometry. The red line shows the shape of the vacuum chamber. A loss peak is observed after the interconnection, at the beginning of the MQ beam screen.
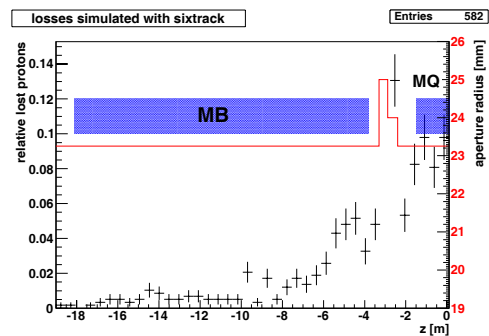
Figure 1: Loss pattern at interconnection between arc magnets simulated using SixTrack code. This loss is generated by halo particles.

The loss pattern to large extent follows the lattice $\beta-$ function. Therefore, almost independent of the mechanism which causes the loss, the highest loss probability is in vicinity of quadrupole magnets where the $\beta-$ function reaches its maximum. In transverse plane the losses are usually concentrated in horizontal or in vertical direction, depending on the onset of the loss phenomena.

The BLM locations have been chosen to minimise the impact of the spatial loss distribution on the BLM thresholds. In case of MB and MQ magnets the impact of the loss distribution on the BLM signal is discussed in [3] and [4].

The temporal distribution of losses has a critical influence on the quench margin of the magnet but also on the signal observed in the BLM due to temporal effects in the analog and digital part of the acquisition system. The ongoing investigations show weak influence of the loss temporal distribution on the quench margin [5]. Losses with a very short rise time are seen in the BLM system with a delay which might in some cases be too large and therefore the beam-abort thresholds needs to be lowered in order to compensate for it.

Quench Margin

For short transient losses (shorter than $100\ \mu s$) the quench margin is estimated through the enthalpy limit of the dry cable, ie. assuming that there is no heat flow from the cable to helium. The specific heat of NbTi superconductor depends on the magnetic field, therefore it varies over the coil. An example of the enthalpy limit map of the coil is presented in Figure 2 for MB magnet at current corresponding to 7 TeV proton beam. The enthalpy limit of the cables is known with a good precision.
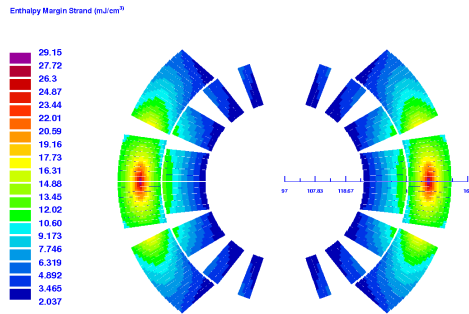
Figure 2: Map of quench margin on the transverse cross-section of the coil for 7 TeV beam energy. The map has been generated by ROXIE code [6].

For steady state losses, which are expected in numerous locations on the LHC, the quench margin is calculated using a thermodynamic model of the heat transfer in the coil and to the cryogenic system [7]. The timescale at which the heat transfer reaches steady-state value is about 1 s.

The magnets are between 5 and 15 meter long and the loss scales are often of the same order. Therefore a significant part of the losses is typically generated nearby the interconnection between two magnets, where a smaller amount of material allows the shower to develop. As a result the endings of the coils can get more energy deposited than the magnet center. Fortunately, the quench margin at the ends of the magnet is expected to be larger than in the middle because of a larger helium content. On the other hand, for ultra-short losses, when helium plays no role in heat evacuation, the situation is less profitable because the bending of the superconducting cable is expected to decrease its enthalpy limit.

For losses with a timescale in between fast and steady state the quench margins can be estimated using a method from [8] or using more precise simulations [5]. These methods are based on the knowledge of the timescale at which various heat transfer processes became active.

Energy Deposition

The distribution of energy deposition in the coil is estimated from particle shower simulations. It is not possible to measure it directly inside the coil, so the only validation of the simulations can be done through quench tests.

For fast losses only the value and the location of the maximum energy deposition are considered. The quench in this case develops in the innermost part of the inner cable, which has the lowest quench margin due to the strongest magnetic field and which is the most exposed to the beam losses.

In case of slower losses the heat is transported along the cables and out to the helium bath. Depending on the approach to the threshold calculation, the relevant parameter is:

- energy deposited averaged over a volume defined by the cable cross section and its transposition pitch [8],

- one-dimensional radial distribution of the energy [5],

- two-dimensional map of energy deposit over the whole cross-section of the coil including the cold bore and the copper wedges [7].

An interesting aspect of the energy distribution in the coil is a distortion of the shower shape due to exceptionally strong magnetic field. This phenomena is illustrated in Figure 3, where the simulation of a 7 TeV proton impacting vertically on the beam screen of the MB magnet is shown. A large part of the cold bore is uniformly heated and the energy deposition in the coil is distorted to the horizontal plane, however shifted towards the loss location. In case of the MB magnet this phenomena shifts the shower away from the most fragile parts of the coil. It decreases the energy deposition and shifts it away from a point critical for the heat evacuation. In case of horizontal loss the magnetic field effect is opposite and leads to energy concentration enhancing the local energy density, as shown in Figure 4.
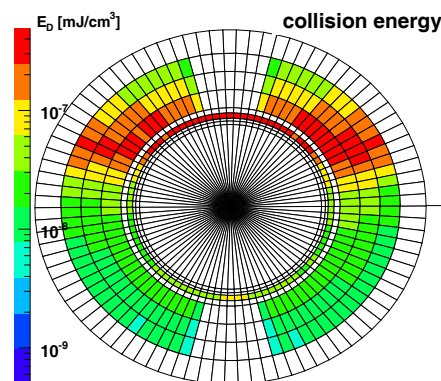
Figure 3: Energy density deposition per lost proton in the cold bore and the inner coil of the MB magnet in case of vertical beam loss as simulated by Geant4. The loss is located on the upper part of the beam screen (not shown on the plot).
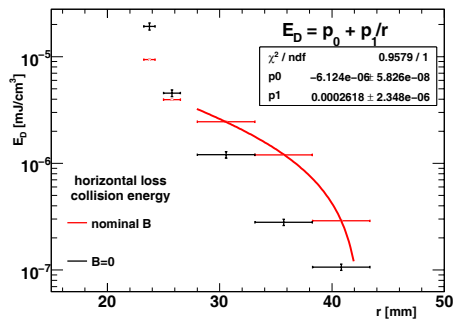
Figure 4: Energy density deposition along the most exposed azimuth. The first bin represents the beam screen, the second - cold bore and the last three bins represent the inner coil of the MB magnet.

BLM Signal

In opposition to energy deposition inside the coil, the BLM signal is not only simulated but also measured. The measurements performed during the second beam-induced quench of a superconducting dipole are shown in Figure 5. The corresponding Geant4 simulation (green line) underestimates the signal by about 50%. The main reason of this discrepancy is probably the precision of modelling of the tail of the shower with Geant4.
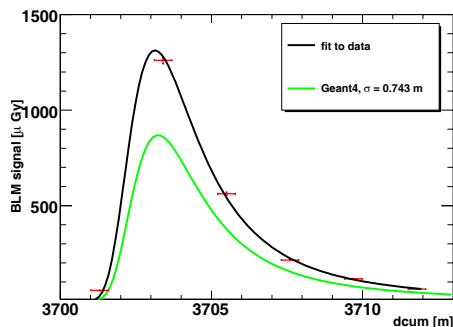
Figure 5: The BLM signal during a beam-induced quench of the MB magnet. Green line shows simulated signal, black line is a fit to the measurements. The quench has been provoked by about $2 \cdot 10^9$ protons with an energy of 450 GeV.

The typical spectrum of the particles reaching the BLM is shown in Figure 6. It is dominated by neutrons, gammas, electrons, positrons and secondary protons. Thermal neutrons, not seen on this plot, are a strong component and to perform the proper simulation of their flux the concrete tunnel walls must be present in the geometry. Convoluting this fluxes with the BLM response functions [9] one obtains the contributions of various radiation types to the BLM signal. The main contribution comes from gammas, pions and protons. The ionisation chamber shows relatively low sensitivity to thermal neutrons [10].

The size of the cascade grows with the distance from the
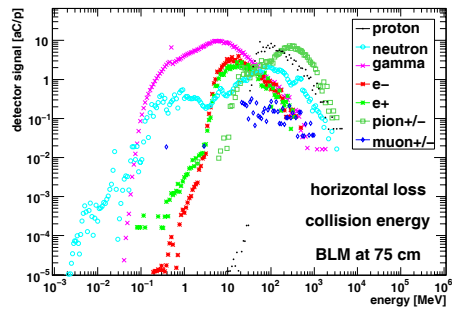
Figure 6: The spectrum of particles reaching the BLM produced by a loss of a single 7 TeV proton.

loss location. It is about 5 times larger outside the cryostat than in the coil, as shown in Figure 7. This leads to the dependence of the threshold on the loss scale. In particular losses due to an obstacle generate smaller ratio of BLM signal to energy deposit in the coil than distributed losses.
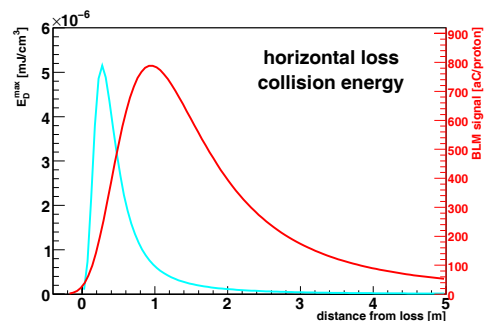
Figure 7: The comparison of longitudinal distributions of energy deposit in the coil and the BLM signal outside the cryostat.

EXAMPLE OF THRESHOLD

The threshold is calculated from the BLM signal Q_{BLM}, the quench margin ΔH and the energy deposited in the coil E_D. In the most general case all these parameters are functions of the beam energy E_b and the time and spatial structure of the loss $\mathcal{L}(t, x, y, s)$.

$$
T(E_b, \mathcal{L}(t, x, y, s)) = \hspace{2cm} (1)
$$
$$
Q_{BLM}(E_b, \mathcal{L}(t, x, y, s)) \frac{\Delta H(E_b, \mathcal{L}(t, x, y, s))}{E_D(E_b, \mathcal{L}(t, x, y, s))}
$$

In the current threshold algorithm the complexity has been reduced removing the weakest dependencies. For instance, as the BLM positions have been chosen to be independent from loss patterns, one can reduce: $Q_{BLM}(E_b, \mathcal{L}(t, x, y, s))$ to $Q_{BLM}(E_b, \tau)$. After all simplifications, the current algorithm can be described as minimisation over beam loss patterns of the Expression 2.

$$T(E_b, \tau) = Q_{BLM}(E_b) \frac{\Delta H(E_b, \tau)}{E_D(E_b, \tau)} \qquad (2)$$

Examples of the threshold tables, each consisting of 384 values, are presented in [11].

TRIPLET CASE

There are a few examples of locations when the signal in the BLM comes not only from loss against which the monitor should be protecting, but also from other radiation sources. Especially interesting case are inner triplet magnets which provide final beam focusing before the interaction points. These magnets are subject to a constant flux of debris from the collisions in the interaction point. These debris are seen as a constant signal and mask the signal coming from the beam loss. This situation is presented in Figure 8 [12].
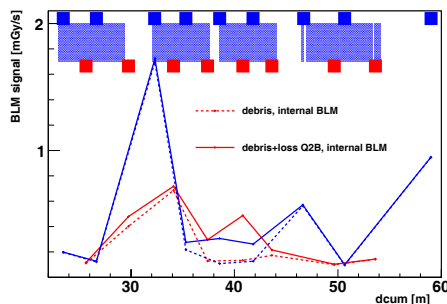
Figure 8: The signal debris (dotted line) and debris plus beam loss signal at quench level, as seen in the BLMs installed on triplet magnets on the right of IP 1.

In this situation it is not possible to determine the thresholds such, that they do not dump the beam during normal operation and, at the same time, they protect the magnets. The solution is to place radiation detectors closer to the coil, inside the magnet cold mass. This solution is being investigated.

BEAM-INDUCED QUENCHES

Since the initial injection tests in summer 2008 until normal operation with intensities up to $5 \cdot 10^{12}$ protons in September 2010 only five beam-induced quenches have occurred. They all were caused by the loss of the injected beam (single-turn failures). In all cases the quenched magnets were main dipoles and the quenches itself were self-recovering when the Quench Protection System heaters, triggered by a voltage spike, fired and safely quenched the whole magnet. Four of these quenches were caused by a vertical loss.

Only the quench level of MB magnet for short transient loss and for injection energy has been tested. The need of systematic quench tests has been stressed by the Machine Protection Panel and the test campaign is foreseen in the fall of 2010.

QUENCH TESTS

To test the quench level at millisecond timescale it is foreseen to use a wire scanner which produces, during scan, a particle shower with well defined properties. It is expected that the MQY magnet placed downstream the wire scanner, should quench when scanning beam with intensity below 10^{13} protons at 3.5 TeV.

Another test of BLM thresholds will be performed producing an orbital bump with a maximum inside the MQ magnet. The magnet chosen to this test is equipped with a special QPS firmware which allows to see signals coming from QPS probes smaller than the quench threshold. It is expected that using this technique quench precursors should be detected without actually quenching the magnet. In the initial stage of this test losses of almost 10^9 protons/meter have been reached but no signal has been observed in QPS.

CONCLUSIONS

The strategy to set up beam-abort thresholds protecting superconducting magnets from quenching is discussed. A few not obvious aspects of the process, as influence of strong magnetic fields on energy deposited in the magnets coils, are emphasized. The simplifications used in the procedure are justified. Special cases, where the protection with the existing system is not possible, are presented. Finally a short summary of the beam-induced quenches observed during the two years of LHC operation is given and the possible quench tests are described.

REFERENCES

[1] C. Zamantzas et al., *An FPGA Based Implementation for Real-Time Processing of the LHC Beam Loss Monitoring System's Data*, Nuclear Science Symposium Conference Record, 2006. IEEE, vol.2, no., pp.950-954

[2] C. Bracco, CERN-THESIS-2009-031.

[3] M. Sapinski, B. Dehning, A. Priebe, *Simulation of Beam Loss in LHC MB magnet and quench threshold test*, CERN-LHC-Project-Note-422.

[4] Ch. Kurfuerst, *Quench Protection of the LHC Quadrupole Magnets*, CERN-THESIS-2010-070.

[5] A. Verweij, private communication, 2010

[6] B. Auchmann, ROXIE Users Documentation, CERN, 2007.

[7] D. Bocian, B. Dehning, A. Siemko, IEEE Transactions on Applied Superconductivity, June 2008.

[8] J. B. Jeanneret, D. Leroy, L. Oberli, T. Trenkler, *Quench levels and transient beam losses in LHC magnets*, LHC Project Report 44, 1996.

[9] M. Stocker, CERN-THESIS-2008-099.

[10] E. Lebbos et al., CERN-EN-NOTE-2010-002-STI

[11] E.B. Holzer, "Commissioning and Optimization of the LHC BLM System", MOPD48, HB2009, Morschach, Switzerland, 2010.

[12] M. Sapinski et al., in preparation